Cell. Mol. Life Sci. (2011) 68:537–551
DOI 10.1007/s00018-010-0470-z

Cellular and Molecular Life Sciences

RESEARCH ARTICLE

Sterol binding by OSBP-related protein 1L regulates late endosome motility and function

Terhi Vihervaara · Riikka-Liisa Uronen · Gerd Wohlfahrt · Ingemar Björkhem · Elina Ikonen · Vesa M. Olkkonen

Received: 12 May 2010 / Revised: 24 June 2010 / Accepted: 14 July 2010 / Published online: 6 August 2010

Abstract ORP1L is an oxysterol binding homologue that regulates late endosome (LE) positioning. We show that ORP1L binds several oxysterols and cholesterol, and characterize a mutant, ORP1L Δ560–563, defective in oxysterol binding. While wild-type ORP1L clusters LE, ORP1L Δ560–563 induces LE scattering, which is reversed by disruption of the endoplasmic reticulum (ER) targeting FFAT motif, suggesting that it is due to enhanced LE–ER interactions. Endosome motility is reduced upon overexpression of ORP1L. Both wild-type ORP1L and the Δ560–563 mutant induce the recruitment of both dynactin and kinesin-2 on LE. Most of the LE decorated by overexpressed ORP1L fail to accept endocytosed dextran or EGF, and the transfected cells display defective degradation of internalized EGF. ORP1L silencing in macrophage foam cells enhances endosome motility and results in inhibition of [^{3}H]cholesterol efflux to apolipoprotein A-I. These data demonstrate that LE motility and functions in both protein and lipid transport are regulated by ORP1L.

Keywords Cholesterol efflux · Endosome motility · Late endosome · Macrophage · Oxysterol · Oxysterol binding protein

Electronic supplementary material The online version of this article (doi:10.1007/s00018-010-0470-z) contains supplementary material, which is available to authorized users.

T. Vihervaara · V. M. Olkkonen (✉)
Minerva Foundation Institute for Medical Research,
Biomedicum Helsinki 2U, Tukholmankatu 8,
00290 Helsinki, Finland
e-mail: vesa.olkkonen@helsinki.fi

T. Vihervaara · V. M. Olkkonen
National Institute for Health and Welfare/Public Health Genomics Unit, Biomedicum 1, 00290 Helsinki, Finland

R.-L. Uronen · E. Ikonen · V. M. Olkkonen
Institute of Biomedicine/Anatomy,
University of Helsinki, P.O. Box 63,
00014 Helsinki, Finland

G. Wohlfahrt
Computer-Aided Drug Design,
Orion Pharma, Orionintie 1, 02101 Espoo, Finland

I. Björkhem
Karolinska Institutet, Karolinska University Hospital Huddinge,
14186 Stockholm, Sweden

Abbreviations

ABCA1	ATP binding cassette transporter A1
acLDL	Acetylated LDL
apoA-I	Apolipoprotein A-I
EGF	Epidermal growth factor
GPF	Green fluorescent protein
ER	Endoplasmic reticulum
GST	Glutathione-*S*-transferase
HDL	High-density lipoprotein
LDL	Low-density lipoprotein
LE	Late endosome
LUV	Large unilamellar vesicle
OHC	Hydroxycholesterol
ORP	OSBP-related protein
OSBP	Oxysterol binding protein
rho	Rhodamine
shRNA	Short hairpin RNA
siRNA	Short interfering RNA
VAP	Vesicle-associated membrane protein-associated protein
WT	Wild-type

Introduction

Oxysterol binding protein (OSBP) was isolated as a cytoplasmic high-affinity receptor for several oxysterols [1–3]. OSBP acts as a sterol sensor that interacts with the endoplasmic reticulum (ER) trans-membrane receptor VAP-A and with PtdIns-4-P in Golgi membranes [4–7]. Binding of 25-hydroxycholesterol (25OHC) to OSBP acts as a signal that is coupled with the function of ceramide transporter (CERT) and thus coordinates the synthesis of sphingomyelin with the cellular sterol status [8]. On the other hand, OSBP acts as a sterol-dependent scaffold for protein phosphatases that dephosphorylate extracellular signal-regulated kinases (ERK; [9, 10]).

Families of proteins displaying sequence homology to OSBP are present throughout the eukaryotic kingdom. These proteins, designated OSBP-related (ORP), OSBP-like (OSBPL) or OSBP homologue (Osh) proteins, have mainly been studied in mammalian and *S. cerevisiae* systems and are shown to be involved in the control of cellular lipid metabolism, vesicle transport, and cell signaling (reviewed by [11–13]. In mammals, the family consists of 12 members [14–16], and in yeast, of 7 members [17].

All ORPs contain in their carboxy-terminal part a structure designated OSBP-related ligand binding domain (ORD), which is homologous to the oxysterol binding domain of OSBP. In addition to the ORD, most ORPs contain an N-terminal region involved in their subcellular targeting. The N-terminal extensions containing a pleckstrin homology (PH) domain target ORP1L to late endosomes (LE) [18], ORP3, -6, and -7 to the plasma membrane [19] and OSBP [5, 20], as well as ORP9 [21] to the Golgi complex. In several cases, the ORP PH domains are known to mediate the binding of phosphoinositides, which is essential for the localization and function of the proteins [5, 6, 22, 23]. A motif called FFAT (two phenylalanines in an acidic tract) mediates binding to the ER resident protein VAP-A and specifies association of a majority of ORPs with ER membranes [24]. The dual targeting signals present on ORPs have prompted the hypothesis that these proteins may act at membrane contact sites occurring between the ER and other organelles [25, 26].

The *OSBPL1* gene encodes two proteins, ORP1L and ORP1S, of which ORP1L is shown to be abundantly expressed in brain, lung and macrophages [18]. This protein localizes to late endosomes (LE), where it forms a tripartite complex with the small GTPase Rab7 and its effector protein Rab7-interacting lysosomal protein (RILP; [18, 27]). This complex plays a key role in the recruitment of dynein–dynactin motor complexes on the surface of LE, resulting in the positioning of LE close to the microtubule minus ends [27–29]. Rocha et al. [30] recently showed that cellular cholesterol depletion or expression of a truncated ORP1L devoid of the entire ORD domain resulted in a shift of LE from a perinuclear to a more peripheral distribution. Furthermore, they provided evidence that ORP1L devoid of the ORD has the capacity to induce contacts between LE and the ER, resulting in a shift of dynein–dynactin from LE surface to VAP-A. Based on these findings, the authors suggested that ORP1L acts as a cholesterol sensor that regulates LE positioning in cells dependent on the lipid composition of LE membranes.

In the present study, we investigate the oxysterol ligand specificity of ORP1L, and show that the protein also binds cholesterol. Via ORP1L overexpression and silencing, we demonstrate that ORP1L controls the actual motility of late endocytic compartments. We provide evidence that ORP1L not only associates with dynactin complexes but also with ones containing the plus-end directed motor kinesin-2. Moreover, ORP1L overexpression is shown to interfere with lysosomal degradation of endocytosed cargo. Finally, we show that ORP1L silencing in macrophage foam cells inhibits the efflux of lipoprotein-derived endocytosed cholesterol to apolipoprotein A-I, providing evidence for the involvement of ORP1L in both protein and lipid transport functions of the late endocytic compartments.

Materials and methods

Antibodies and other reagents

The rabbit ORP1L antibody R247 used for western analyses was described in [23]. Anti-ORP1L R285 for immunofluorescence analysis was generated by immunizing New Zealand White rabbits with a GST fusion protein carrying aa 1–237 of ORP1L, and affinity purified with the same antigen coupled to CNBr-Sepharose 4B (GE Healthcare, Little Chalfont, Buckinghamshire, UK). A monoclonal mouse antibody (mab) against Xpress epitope tag was purchased from Invitrogen (Carlsbad, CA, USA), lysosome-associated membrane protein-1 (Lamp-1) antibody against mouse (ID4B) or human (H4A3) protein was from Santa Cruz Biotechology (Santa Cruz, CA, USA), and mab against early endosome antigen-1 (EEA-1) was from BD Transduction Laboratories (San Jose, CA, USA). Mabs against KIF3A and $p150^{glued}$ were from BD Transduction Laboratories. Rabbit polyclonal antibody against actin was from Santa Cruz. All fluorescent secondary antibodies and fluorescent markers were from Invitrogen–Molecular Probes.

cDNA constructs and shRNA lentiviruses

cDNA constructs pGFP-ORP1L, pcDNA HisMaxC-ORP1L, pGFP-Rab7, and pGFP-RILP were described in [31].

QuikChange® II Site-Directed Mutagenesis Kit (Stratagene, La Jolla, CA, USA) was used for deletion of amino acids 560–563 (ELSK) in ORP1L sequence. To disrupt the FFAT motif in ORP1L, amino acids 475–479 (EFYDA) were mutated to EVVVA.

shRNA lentiviruses were purchased from Sigma MISSION® TRC-Mm 1.0 (Mouse) shRNA library, shORP1L.1 corresponds to TRCN0000105072 and shORP1L.2 to TRCN000010573. Human ORP1L siRNA duplexes with sense strand sequence 5′-UrGrCrCrArGUrGrCrCrGrGrAU UrCUrGrATT-3′ were obtained from Sigma-Aldrich (St. Louis, MO, USA).

Homology modeling of human ORP1

The amino acid sequences of all human and mouse ORP proteins as well as those from *S. cerevisiae* were used to construct a multiple sequence alignment with ClustalW (version 1.82) [32]. The structure of yeast Osh4p [33] was used as a template for modeling the C-terminal part of human ORP1L. Prime 1.6 (Schrödinger LLC, Portland, OR, 2007) was used to align the ORP1L sequence with Osh4p (PDB code 1zhx) obtained from the PDB www.pdb.org, [34]. Corrections to this alignment were introduced manually, taking the positions of secondary structure elements in the template and the Hidden Markov Model consensus sequence obtained with HMMER/Pfam (integrated into Prime 1.6) into account. The overall sequence identity between ORP1L and the structural template Osh4p is ∼24%; the putative sterol binding pocket exhibits a slightly higher degree of conservation than the rest of the protein. The N-terminal region was omitted from the alignment and the final structural model of ORP1L consists of amino acids S539 to Y950, which corresponds to the sequence of the shorter ORP1S, except for its first 25 amino acids. Prime 1.6 was used to build loops for three insertion and six deletion regions, and after this, new side chains were placed and their conformations optimized. 25OHC was taken from the template 1zhx and its position was adjusted in the final minimization of the complete model.

Cell culture and transfection

HeLa cells were cultured in DMEM (Sigma) supplemented with 10% FBS, 20 mM Hepes, 100 U/ml penicillin, and 100 μg/ml streptomycin. The cells were transfected with DNA using Lipofectamine 2000 (Invitrogen) according to the manufacturer's instructions. HiPerFect (Qiagen, Alameda, CA, USA) reagent was used for siRNA transfections.

Mouse macrophage RAW264.7 cells were cultured in DMEM supplemented with 10% FBS, 10 mM Hepes, 100 U/ml penicillin, 100 μg/ml streptomycin. Lentiviral transduction was performed according to the manufacturer's (Sigma) instructions, and selection was carried out using puromycin (4 μg/ml).

Recombinant protein production and in vitro sterol binding assays

Glutathione-*S*-transferase (GST) fusion proteins of ORP1L and -S were produced in *E. coli* and purified using Glutathione-Sepharose 4B (GE Healthcare). Protein concentrations were determined by the DC assay (BioRad, Hercules, CA, USA) and protein amounts were equalized with the help of Coomassie Blue stained SDS PAGE. In vitro oxysterol binding assays were performed as described in [35], and cholesterol binding as in [36].

Fluorescence microscopy and image analysis

For time lapse fluorescence microscopy, cells were imaged using a Zeiss LSM5 Live microscope in CO_2 independent medium (Gibco/Invitrogen). Motility was quantified using Image Pro Plus software (Media Cybernetics). For analyzing epidermal growth factor (EGF) degradation, HeLa cells were incubated in DMEM supplemented with 2 mg/ml BSA and 10 mM Hepes (pH 7.4) for 1 h at 37°C. The cells were then incubated with rhodamine-labeled EGF (Molecular Probes) at 200 ng/ml for 1 h, washed three times with the BSA containing medium, and incubated further up to 6 h before fixation in 4% PFA and fluorescence microscopy analysis. Immunofluorescence microscopy was performed as described in [27]. The specimens were viewed using a Leica SP2 confocal microscope. Fluorescence image processing and quantitation was performed with Adobe Photoshop and ImageJ softwares.

Analysis of cellular [^{3}H]cholesterol efflux

Preparation of acetylated LDL and its radiolabeling were performed as previously described [37, 38]. ORP1L silenced cells were seeded and loaded with 25 μg/ml [^{3}H]cholesterol oleate containing acLDL in DMEM containing 5% lipoprotein deficient serum and antibiotics. After 48 h loading, cholesterol was effluxed for 16 h to serum-free medium containing antibiotics, with or without lipid-free human apolipoprotein A-I (apoA-I;10 μg/ml) or HDL_2 (25 μg/ml) as cholesterol acceptor.

Analysis of cellular free and esterified cholesterol

RAW264.7 cells were loaded with [^{3}H]cholesterol oleate acLDL as above. After washing with PBS, lipids were extracted and analyzed by thin-layer chromatography as described earlier [39].

Other methods

Coimmunoprecipitation was performed as described in [31]. Quantitative real-time PCR (qPCR) was performed as described earlier [40] with the following primers: ORP1L-forward GTCTAACTTGGGCTGGACACC, ORP1L-reverse CAGCTCCTTTCGTCCTGTGAAG, housekeeping gene 36B4-forward CATGCTCAACATCTCCCCCTT, 36B4-reverse GGGAAGGTGTAATCCGTCTCCACAG.

Results

ORP1L binds several oxysterols and cholesterol

ORP1L has been reported to bind 22(R)- and 25-hydroxycholesterol (OHC) [41, 42]. To further investigate the ligand specificity of ORP1L, we analyzed the ability of a number of oxysterols to compete the binding of [^{3}H]-25-hydroxycholesterol ([^{3}H]-25OHC), in an in vitro charcoal dextran-based assay employing purified recombinant GST-ORP1L (500 nM). A constant 40 nM concentration of [^{3}H]-25OHC could be competed with 1- to 50-fold excess of 7-ketocholesterol, 22(R)OHC, 24(S)OHC, and 25OHC (Fig. 1a). The different unlabeled oxysterols competed the [^{3}H]-25OHC binding with approximately equal efficiency, with no statistically significant differences between the binding curves.

In addition to several oxysterols, ORP1L has been suggested to bind cholesterol [30, 41]. To investigate the capacity of ORP1 to bind cholesterol, we employed an assay measuring the ability of a protein to extract [^{3}H]cholesterol from large unilamellar phosphatidylcholine-cholesterol vesicles (LUV). Since we were unable to purify GST-ORP1L from *E. coli* in the absence of detergent, residues of which in protein preparations disturb the integrity of the LUV, we used for this purpose GST-ORP1S [18, 43] encompassing the ligand binding domain of the protein. The results show protein concentration-dependent extraction of the [^{3}H]cholesterol by GST-ORP1S, similar to that observed for ORP2 used as a positive control (Fig. 1b; [35]).

Sterol binding deficient ORP1L

To elucidate the role of sterol binding for ORP1L function, we generated a sterol binding mutant of ORP1L by deleting four amino acids (ELSK, amino acids 560–563) from the ORP1L sterol binding domain. Deletion of this region has been shown to result in a deficiency of sterol binding in other ORP family members [8, 36, 44]. Homology modeling of the ORP1L ligand binding domain (Fig. 1c) suggests that this deletion (highlighted in blue) localizes in the lid region, and a leucine residue (L561) in this region is in direct hydrophobic interaction with the sterol side chain. We employed the in vitro binding assay with purified recombinant protein to show that this mutant is severely defective in binding 22(R)-, 24(S)-, or 25OHC (Fig. 1d–f). We thus concluded that the mutant is a good tool to study the role of ORP1L ligand binding in the function of the protein.

Specific inactivation of ORP1L sterol binding inhibits ORP1L-induced LE clustering

ORP1L has been shown to localize on LE and overexpression of the protein clusters endosomes in the perinuclear area of the cell [18]. The LE clustering has been linked to increased dynein–dynactin motor complex activity, which is recruited to LE by an effector complex comprising of Rab7 GTPase, ORP1L, and Rab7 interacting lysosomal protein, RILP [27].

To investigate the subcellular localization of the sterol binding-deficient mutant ORP1L Δ560–563, HeLa cells were transfected with Xpress-tagged ORP1L and GFP-tagged Rab7 cDNAs, and the expressed proteins were visualized by confocal fluorescence microscopy. While WT ORP1L induced LE clustering clearly distinct from the normal LE distribution (Fig. 2A), overexpression of ORP1L Δ560–563 resulted in scattered localization of the organelles (Fig. 2B, a). The identity of ORP1L Δ560–563 positive organelles was characterized by immunofluorescence analysis using co-staining for the endogenous early or late endosomal markers EEA-1 or LAMP-1, respectively. ORP1L Δ560–563 did not colocalize with EEA-1 (Fig. 2B, d–f), but colocalized partially with LAMP-1 (Fig. 2B, g–i), similarly to WT ORP1L [23]. Both the WT and mutant ORP1L-positive structures colocalized extensively with GFP-Rab7 (Fig. 2A, B). We also monitored the localization of WT ORP1L and the Δ560–563 mutant in the RAW264.7 macrophage model. Similarly to results in HeLa cells, in the macrophage WT ORP1L was found on perinuclear clusters of endosomal elements, while the Δ560–563 mutant decorated endosomes with a scattered distribution. As in the HeLa cells, the structures colocalized partially with Lamp1 (Fig. S1).

ORP1L forms a physical complex with Rab7 [23]. To investigate the possibility that the Δ560–563 mutant might have a defect in Rab7 interaction, we compared the ability of WT and mutant ORP1L to co-immunoprecipitate Rab7. No difference was detected in the Rab7 interaction of the two proteins (Fig. 2D).

Rocha et al. [30] recently suggested a model where ORP1L acts as a sensor of cholesterol levels in the LE and operates at LE–ER contact sites. In the absence of bound ligand, ORP1L adopts a conformation where it is bound to the ER protein VAP through its FFAT motif, resulting in a peripheral distribution of LE. When cholesterol level rises,

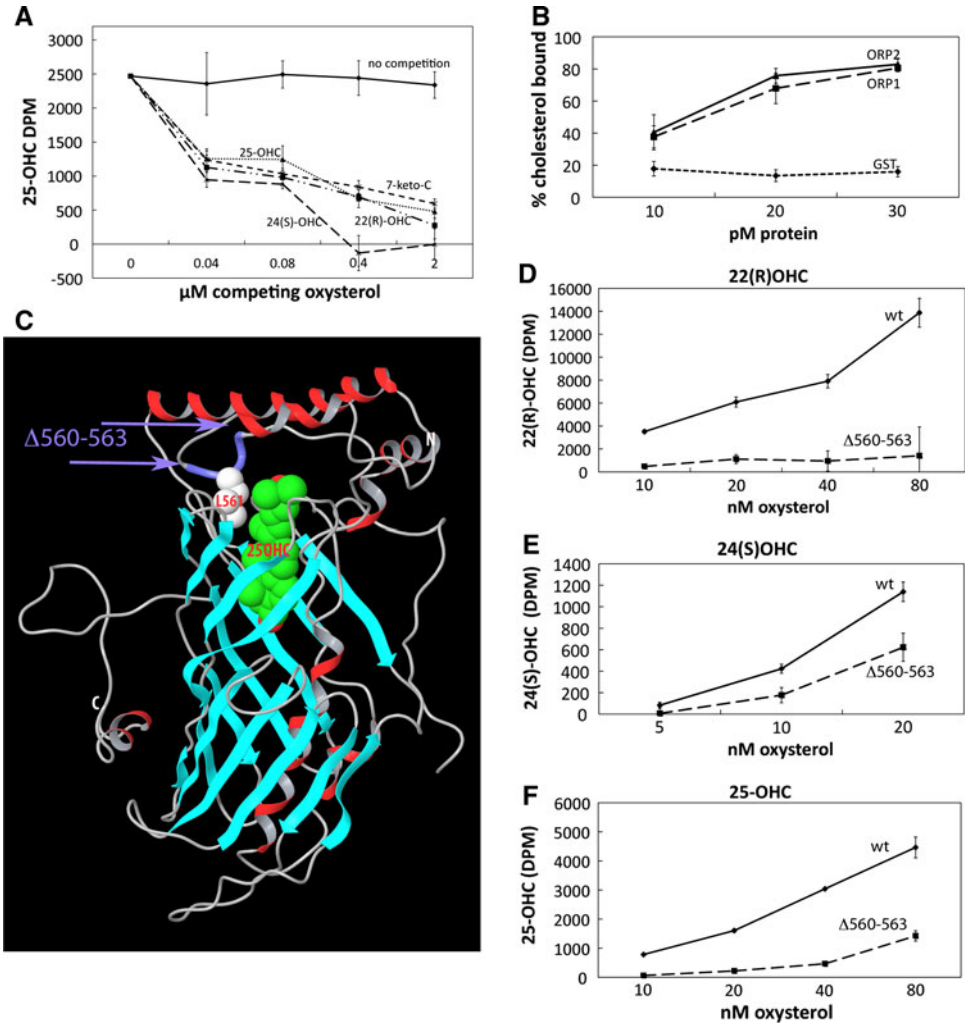

Fig. 1 ORP1L binds several oxysterols and cholesterol in vitro. **a** Binding of [^{3}H]25OHC (40 nM, *y*-axis: bound DPM) by purified ORP1L can be competed with increasing concentrations (indicated at the *bottom*) of 7-ketocholesterol, 22(R)OHC, and 24(S)OHC. **b** The ORP1 sterol binding domain (ORP1) extracts [^{3}H]cholesterol from LUVs composed of phosphatidylcholine and 1 mol% cholesterol. ORP2 was included as positive and plain GST as negative control. **c** A molecular model of ORP1 sterol binding domain with bound 25OHC (in *green*) in the pocket. The region of four amino acids (Δ560–563) that are deleted in the sterol binding deficient mutant Δ560–563 is highlighted in *purple*. This region contains a leucine residue (L561, side chain indicated in *white*) that is predicted to directly interact with the sterol side chain. **d–f** The sterol binding-deficient mutant ORP1L Δ560–563 is deficient in binding 22(R)-, 24(S), or 25-hydroxycholesterol. The data in (**a**, **b**, **d–f**) represent mean ± SEM ($n = 3$)

a conformational change occurs in ORP1L abolishing the interaction with VAP, and LE cluster in the perinuclear area. To test this hypothesis, we mutated the FFAT motif in ORP1L Δ560–563 to see if specific inactivation of VAP binding would affect the localization of ORP1L positive organelles. When overexpressed in HeLa cells, the ORP1L Δ560–563 mFFAT double mutant clustered to the perinuclear region very efficiently, indicating that the LE scattering by the Δ560–563 mutant is indeed caused by interaction with the ER in the cell periphery (Fig. 2C, a–c).

ORP1L induces recruitment of both plus- and minus end-directed motor proteins on LE

To investigate if the scattered localization of LE induced by ORP1L Δ560–563 resulted from inability of the protein to recruit dynein–dynactin motor complexes, transfected HeLa cells were double-stained for different members of the Rab7-RILP-ORP1L complex or for dynein subunit p150^{glued}. ORP1L Δ560–563 colocalized with Rab7 (Fig. 2A, d–f), RILP (data not shown) and p150^{glued} (Fig. 3a) similarly to WT ORP1L. The fact that ORP1L Δ560–563 induced the recruitment of the dynein–dynactin subunit p150^{glued} to the surface of LE just as efficiently as WT ORP1L, led us to investigate whether ORP1L could affect other motor proteins. Scattering of ORP1L Δ560–563 positive LE in the cell periphery brought up the possibility that, in addition to LE contacts with the ER, a plus-end directed motor protein might be involved. Therefore, HeLa cells overexpressing ORP1L were stained for the endogenous kinesin-2 motor protein subunit KIF3A, which has been shown to regulate LE movement in a plus-end directed manner [45]. Confocal microscopy analysis revealed that in HeLa cells kinesin-2 was recruited to the surface of ORP1L positive LE in the case of both WT and sterol binding-deficient proteins (Fig. 3b). Both p150^{glued} and KIF3A displayed a cytosolic-appearing distribution in untransfected cells (Fig. 3c). These results suggest that the modulation of microtubule-dependent positioning of LE by ORP1L does not only involve minus-end directed motor proteins but also plus-end directed ones. No evidence for a physical interaction between ORP1L and KIF3A could be

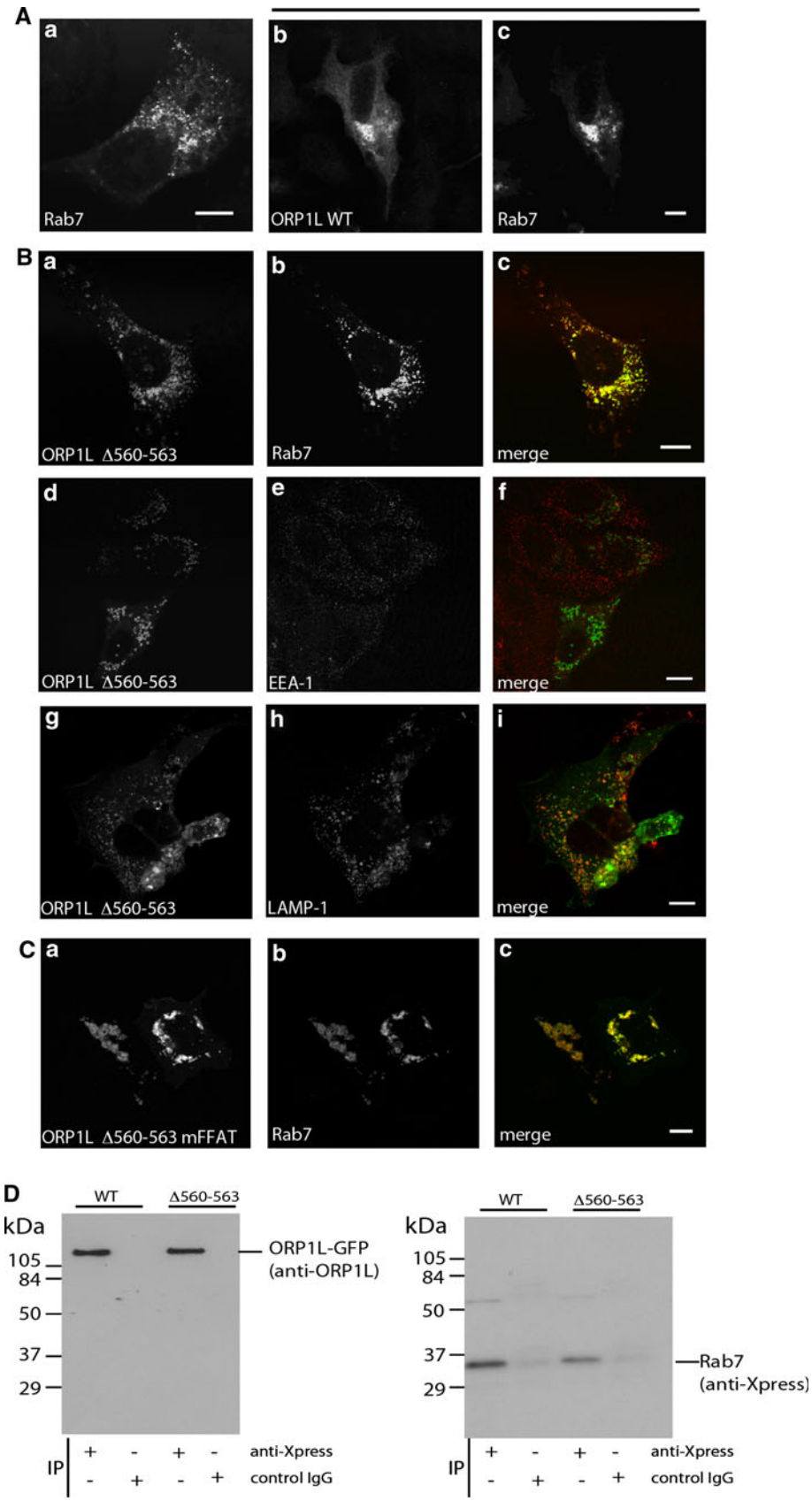

Fig. 2 Subcellular localization and Rab7 interaction of ORP1L Δ560–563. **A** LE positioning in HeLa cells. (*a*) Localization of Rab7 positive organelles in the absence of ORP1L overexpression. (*b–c*) Overexpression of WT ORP1L results in clustering of Rab7 positive late endosomes close to the nucleus. **B** (*a–c*) Overexpression of ORP1L Δ560–563 results in a scattered distribution of LE, the organelles colocalizing extensively with Rab7. (*d–f*) ORP1L Δ560–563 does not colocalize with the early endosomal marker EEA-1, but (*g–i*) colocalizes partly with Lamp-1. **C** (*a–c*) Disruption of the FFAT motif in ORP1L Δ560–563 rescues the LE clustering phenotype in cells expressing ORP1L Δ560–563 mFFAT. *Bars* 10 μm. **D** Both WT and Δ560–563 ORP1L coimmunoprecipitate with Rab7 GTPase. HeLa cells were double transfected with GFP-ORP1L and Xpress-Rab7, followed by immunoprecipitation with anti-Xpress or control IgG (*bottom*), and western blotting with ORP1L and Xpress antibodies (*right*)

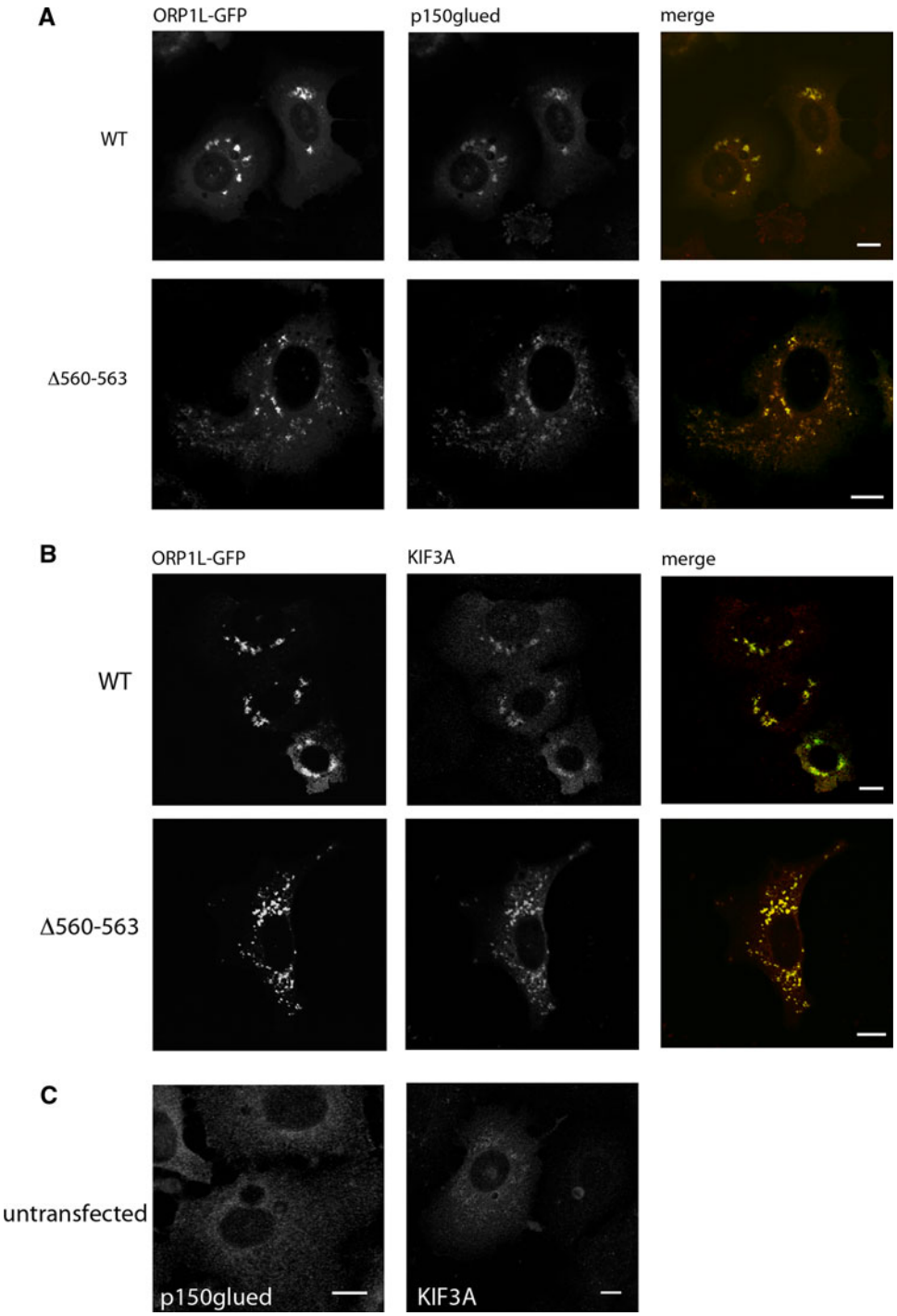

Fig. 3 ORP1L recruits both plus- and minus-end directed motor proteins on LE. **a** HeLa cells transfected with GFP fusions of WT ORP1L or the Δ560–563 mutant were stained for endogenous $p150^{glued}$ (**a**) or KIF3A (**b**). Despite the totally different distribution of LE decorated by WT ORP1L and the Δ560–563 mutant, both proteins accumulate the dynactin subunit $p150^{glued}$ (**a**) and the kinesin-2 subunit KIF3A (**b**) to the LE surface. The distributions of $p150^{glued}$ and KIF3A in untransfected cells are displayed in (**c**). *Bars* 10 μm

obtained by immunoprecipitation (data not shown). We therefore assume that the interaction is indirect, possibly mediated via Rab7, RILP, and dynactin.

ORP1L overexpression disturbs LE/lysosome motility

To determine the effect of ORP1L on the actual motility of late endocytic compartments, HeLa cells were transfected with GPF-tagged WT ORP1L, ORP1L Δ560–563, ORP1L mFFAT, the double mutant ORP1L Δ560–563 mFFAT, or empty vector. The cells were incubated overnight with fluorescent Alexa568-dextran to label late endocytic compartments, and the organelle motility was monitored with live cell confocal microscopy. The analysis revealed that the average motility of Alexa568-dextran labeled compartments was significantly decreased in cells overexpressing ORP1L or any of its mutant forms (Fig. 4a, red bars; Supplemental videos 1–5). The organelles positive for ORP1L WT,

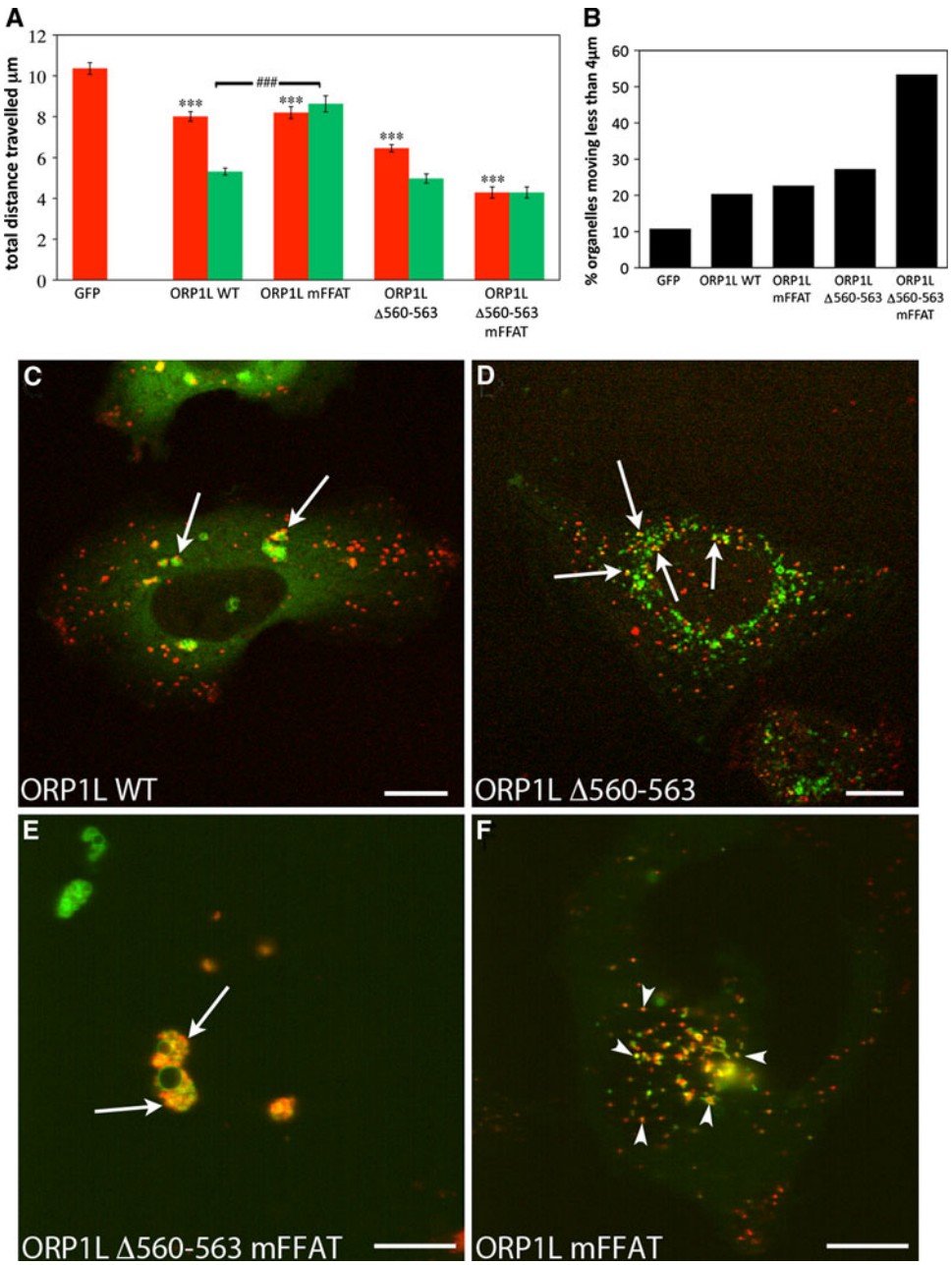

Fig. 4 ORP1L overexpression reduces endosomal motility. **a** Live cell microscopy analysis (1 frame/s, 1 min total) reveals that overexpression of GFP-tagged ORP1L in HeLa cells decreased the total distance travelled by Alexa568-dextran labeled LE/lysosomes (*red bars*). The motility of ORP1L positive compartments is indicated as *green bars*. **b** The proportion of immotile or low motility endosomes was increased in cells overexpressing ORP1L or its mutant forms. The data in **a** and **b** represent **a** quantification of the total distance travelled by the organelles in 1 min or **b** the percentage of compartments travelling <4 µm total distance in 1 min (mean ± SEM, $n = 100$–200 organelles; $^{###}/^{***}P < 0.001$). Some of the endosomes were attached on the surface of ORP1L-positive immotile structures. The phenomenon is illustrated in snapshot images (**c**–**f**) from videos, in which Alexa568-dextran endosomes (*red*) stuck on the surface of ORP1L-positive compartments (*green*) are indicated with *arrows*. **f** A lot of the endocytosed dextran was found within the ORP1L mFFAT positive endosomes, indicated with *arrowheads*. *Bars* 10 µm

Δ560–563, or the double mutant Δ560–563 mFFAT (Fig. 4a, green bars) showed a markedly low motility. Intriguingly, the ORP1L mFFAT containing endosomes were significantly more motile than the other constructs. Moreover, the proportion of immotile or low motility endosomes was increased in cells expressing any of the ORP1L constructs, but especially the double mutant Δ560–563 mFFAT (Fig. 4b). We also observed that overexpression of ORP1L had a global effect on endosome motility (data not shown), not only on the structures decorated by the protein. The impaired movement of endo-lysosomes that carry no detectable ORP1L on their surface may be due to sequestration of factors, such as Rab7 or motor proteins, required for normal endo-lysosome motility, thus reducing their availability for other organelles.

Intriguingly, Alexa568-dextran colocalized very little with large ORP1L containing endosome clusters, an observation also reported earlier [23]. Even though the ORP1L positive structures were mostly dextran negative, dextran positive organelles were often attached to the surface of ORP1L (Fig. 4c) or ORP1L Δ560–563-positive compartments (Fig. 4d). This phenomenon was enhanced by the double mutant Δ560–563 mFFAT, where the majority of the dextran was associated with the hyper-clustered ORP1L endosomes (Fig 4e). However, in the

case of ORP1L mFFAT, the majority of the endocytosed dextran reached the motile ORP1L endosomes, suggesting that the motility of the ORP1L mFFAT endosomes facilitates their communication with organelles carrying the internalized tracer (Fig. 4e; Supplemental video 5).

Endosomal motility is enhanced in ORP1L silenced cells

To analyze how reducing the cellular amount of ORP1L affects endosome motility, we quantified the motility of Alexa568-dextran-labeled compartments in HeLa cells treated with ORP1L-specific or non-targeting control siRNA (Fig. 5a). The silencing efficiency was 75–80%. In ORP1L silenced cells, the motility of endo-lysosomes was significantly increased (Fig. 5b). This effect is opposite to that of ORP1L overexpression, and supports the role of ORP1L as a physiological regulator of LE motility. In addition to the increased motility of endo-lysosomes in ORP1L silenced cells, we found that LE spent more time in the cell periphery in siORP1L-transfected cells (Fig. 5c) as compared to the controls (Fig. 5b). This is consistent with a role of ORP1L in regulating the balance of motor proteins functional on the LE.

Next, we assessed the role of endogenous ORP1L in the function of RILP with an established role in the recruitment of dynein/dynactin and in perinuclear LE clustering. Cells treated with control or ORP1L siRNAs were transfected with GFP-RILP and LE were labeled overnight with Alexa568-dextran. Confocal microscopy analysis revealed that silencing of ORP1L (Fig. 5a) did not inhibit the LE/lysosome clustering induced by GFP-RILP (Fig. S2A). This result is somewhat contradictory to that of Johansson et al. [27] and demonstrates that normal levels of ORP1L are not required for dynein/dynactin recruitment on LE by RILP. Moreover, we tested whether the Δ560–563 mutant inhibits the RILP-induced LE clustering. We found that the mutant protein completely abolished the LE centralization by RILP (Fig. S2B), similarly to the truncated ΔORD construct in the study of Rocha et al. [30].

ORP1L overexpression disturbs endocytic pathway function

To investigate whether overexpression of ORP1L has an effect on the endocytic pathway function, we used a fluorescent degradable marker, rhodamine epidermal growth factor (rhoEGF), which was internalized into either ORP1L

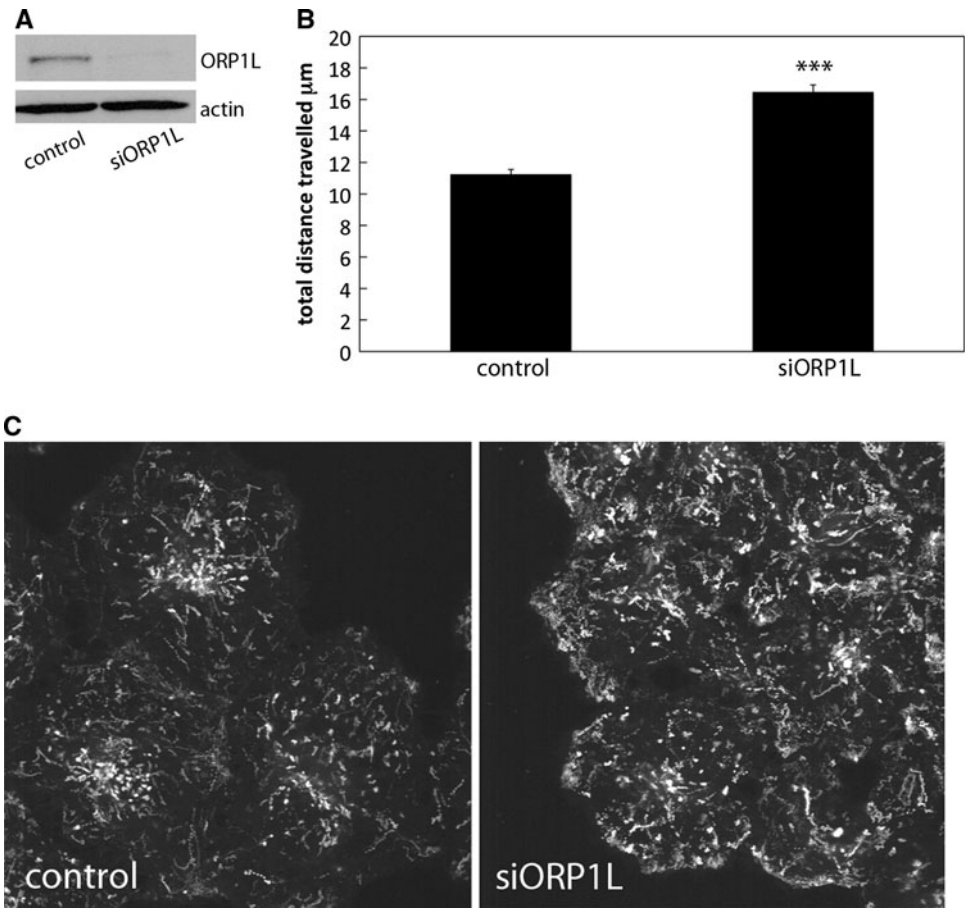

Fig. 5 ORP1L silencing increases endosomal motility. **a** Western blot analysis of ORP1L in HeLa cells at 72 h after siRNA transfection with non-targeting (*control*) or ORP1L-specific (*siORP1L*) siRNAs. **b** Live cell microscopy analysis (1 frame/s, 1 min total) of endosomes in siRNA-treated cells labeled overnight with Alexa568-dextran. The endosomal motility is significantly enhanced by ORP1L silencing. Total distance traveled by the labeled endosomes is depicted (mean ± SEM; $n = 100$–200 organelles; $^{***}P < 0.001$). **c** Trajectory figures from control or siORP1L transfected cells reveal altered endosome tracks in ORP1L-silenced cells. While the movement of endosomes in control cells concentrated in the perinuclear region, the endosomes in ORP1L silenced cells spent more time in the cell periphery. *Bars* 10 µm

or mock-transfected HeLa cells for 1 h, and monitored the degradation of EGF in these cells. After a 4-h chase, there was practically no EGF visible in control cells, but approximately 30% of the WT ORP1L and 40% of the ORP1L Δ560–563 overexpressing cells had a bright EGF signal (Fig. 6a). In cells overexpressing ORP1L, rhoEGF accumulated in relatively large vesicles, many of which were positive for LAMP-1, and showed no colocalization with the early endosome marker EEA-1 (Fig. S3). These vesicles did not contain detectable amounts of ORP1L (Fig. 6d–e), suggesting an indirect effect of ORP1L overexpression on rhoEGF degradation. This could reflect a defect in the ability of LE containing endocytosed cargo to transport their cargo to lysosomes, and is consistent with the earlier finding of Johansson et al. [23] that internalized fluorescent dextran failed to reach Lamp1-positive compartments decorated by overexpressed ORP1L.

To determine the effect of ORP1L silencing on rhoEGF degradation, rhoEGF was internalized into HeLa cells transfected either with non-targeting control or ORP1L-specific siRNA, and the amount of cellular fluorescence was quantitated at different time points. The rate of rhoEGF degradation did not differ between the control and siORP1L treated cells, the latter of which, however, displayed a somewhat enhanced uptake of the tracer (Fig. 6b). These results suggest that the degradative function of the late endocytic pathway is sensitive to ORP1L overexpression but not to reduction of its cellular level.

Silencing of ORP1L in macrophages increases the motility of DiI-acLDL labeled endo-lysosomes and inhibits cholesterol efflux to apolipoprotein A-I

ORP1L has been shown to be upregulated when monocytes mature into macrophages [18]. LDLr knockout mice that received bone marrow cells from transgenic mice expressing human ORP1L under SR-A promoter were shown to have increased atherosclerotic lesion size [42], suggesting a role for ORP1Lin atherogenesis. Macrophage foam cells are thus an important model to study the function of ORP1L.

To investigate whether ORP1L silencing impacts the motility of endosomes also in macrophage foam cells we used fluorescently labeled acLDL. We generated RAW264.7 cell pools stably expressing control or two independent ORP1L shRNAs. In the ORP1L silenced cell pools, shORP1L.1 and shORP1L.2, the ORP1L mRNA expression was reduced by approximately 75%, as determined

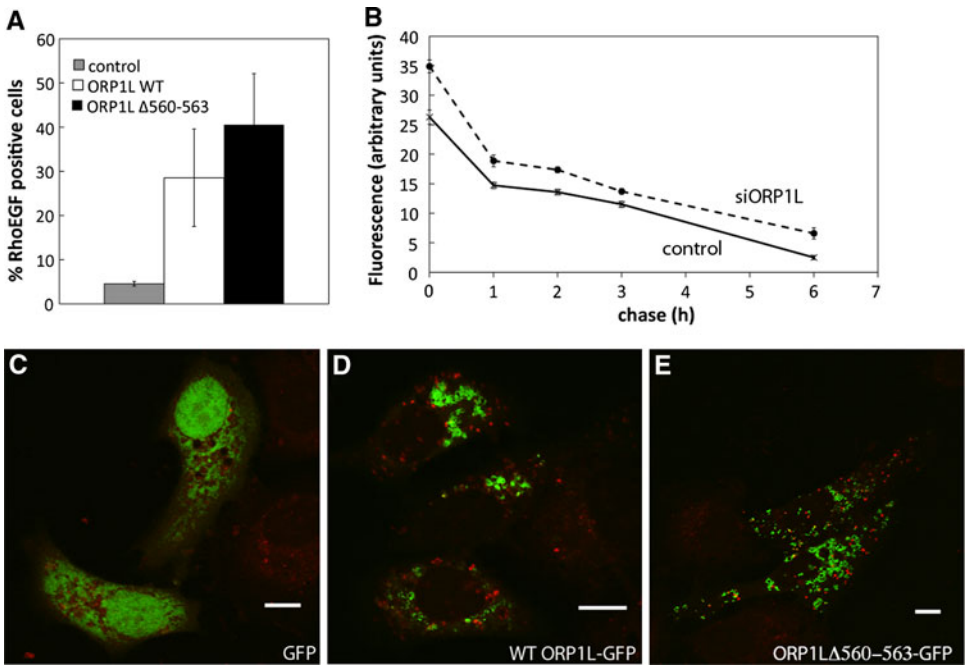

Fig. 6 ORP1L overexpression inhibits the degradation of rhodamine EGF. **a** Rhodamine EGF was internalized in HeLa cells transfected with WT ORP1L (*white bar*), ORP1L Δ560–563 (*black bar*), or the empty vector plasmid (*gray bar*), and disappearance of the intracellular rhoEGF was quantified after 4 h. ORP1L significantly inhibited rhoEGF degradation compared to the mock-transfected cells. The result represents a mean (±SEM) from three different experiments where 100 transfected cells were monitored for positive EGF signal. **b** Silencing of ORP1L does not affect rhoEGF degradation. rhoEGF degradation as a function of time was determined by quantifying the fluorescence from nearly confluent coverslips using the same microscopic settings. The results represent a mean (±SEM) of >10 individual frames. **c–e** Fluorescence microscopy visualization of the internalized rhoEGF in mock transfected or ORP1L overexpressing cells. The mock (GFP) transfected cells did not contain significant rhoEGF signal after four chase, whereas rhoEGF accumulated in WT ORP1L or Δ560–563 expressing cells in vesicles that did not significantly colocalize with ORP1L. *Bars* 10 μm

with qPCR. Silencing at the protein level was additionally confirmed by western blotting (Fig. 7a). Control and ORP1L silenced RAW264.7 macrophages were incubated with DiI-acLDL (50 μg/ml for 1 h), followed by live cell imaging. We found that in ORP1L silenced cells, the DiI-acLDL containing organelles displayed increased motility as judged by the more readily visualized vectorial organelle trajectories in ORP1L silenced versus control cells (Fig. 7a; Supplemental videos 6–8).

To study the contribution of endogenous ORP1L to macrophage cholesterol efflux, the control and ORP1L-silenced cells were loaded with [^{3}H]cholesterol ester-labeled acetylated LDL and the efflux of [^{3}H]cholesterol to apolipoprotein A-I (apoA-I) and high density lipoprotein (HDL_2) was measured. ORP1L silencing inhibited cholesterol efflux to apoA-I (shORP1L.1, 25%; shORP1L.2, 39%) but not to HDL_2 (Fig. 7b). ORP1L silencing had no effect on the cellular uptake [^{3}H]CE-acLDL (data not shown). Furthermore, inhibition of cholesterol efflux was only detected when cells were labeled using [^{3}H]CE-acLDL internalized via scavenger receptor-mediated endocytosis, not when free [^{3}H]cholesterol was used for the labeling. These results suggest that the endogenous ORP1L is involved in endosomal cholesterol transport, and that an ATP binding cassette transporter A1 (ABCA1) mediated cholesterol efflux pathway is specifically affected. No significant difference in the free [^{3}H]cholesterol/cholesterol ester ratio was detected between ORP1L overexpressing or silenced and control cells (data not shown), suggesting that the observed inhibition of [^{3}H]cholesterol efflux was not due to a defective hydrolysis of [^{3}H]cholesterol esters.

Discussion

In the present study, we report novel information on the ligand binding properties of ORP1L and on the functional role of the ORP1L ligand interaction. The data show that

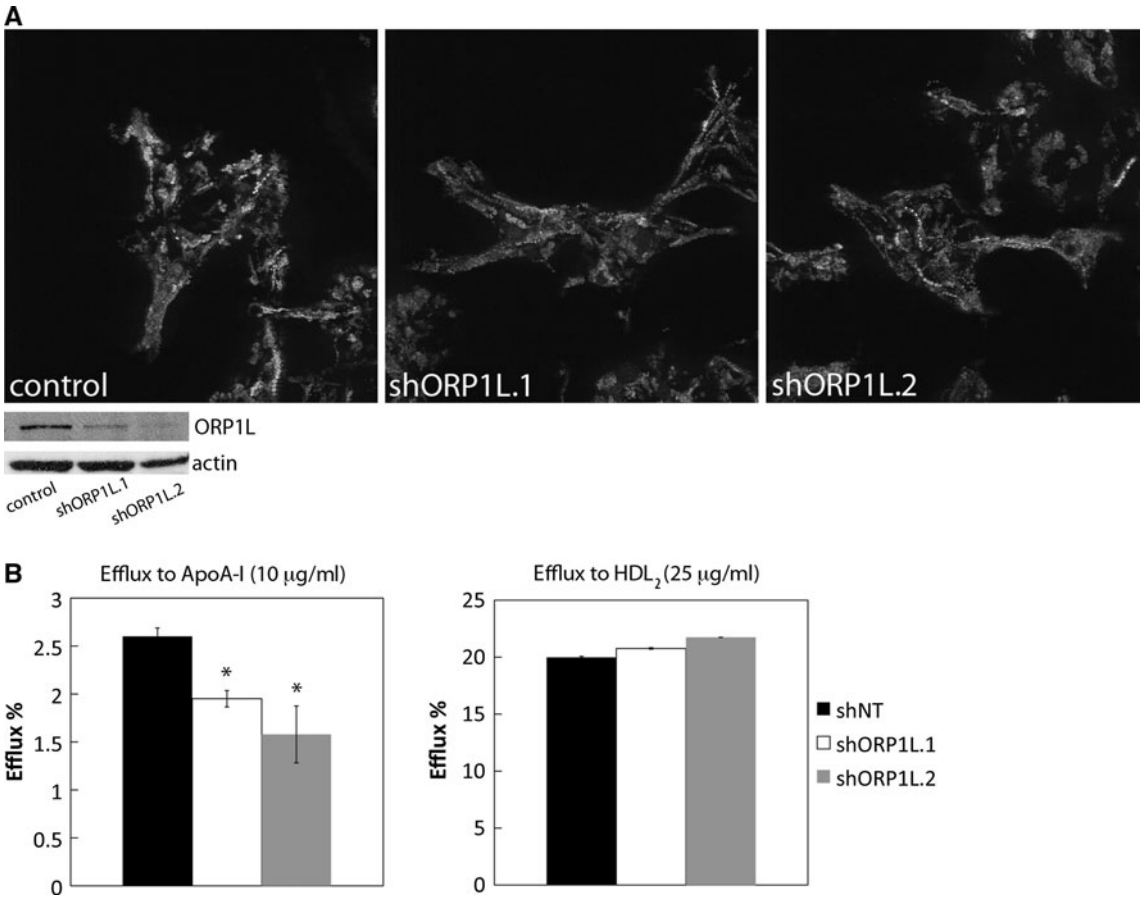

Fig. 7 Silencing of ORP1L in RAW264.7 macrophage increases endosome motility and inhibits cholesterol efflux. **a** RAW264.7 cells transduced with the indicated shRNA lentiviruses and incubated with DiI-acLDL to label late endocytic compartments were imaged at 2 frames/s for 20 s. Sequential frames were subtracted and the resultant images stacked to create a picture showing only the moving pixels. Western analysis of lentivirally transduced RAW264.7 cells expressing control or ORP1L-specific shRNAs is shown. **b** Lentiviral silencing of ORP1L with two independent ORP1L shRNA resulted in significant reduction in cholesterol efflux to ApoA-I, but not to HDL_2. The result represents a mean (±SEM; $n = 3$; $^*P < 0.05$)

ORP1L binds a spectrum of oxysterols, similar to the founder member of the ORP family, OSBP [1]. Of the oxysterols shown to bind to ORP1L, 7-ketocholesterol represents a species abundant in human atherosclerotic lesions and macrophage foam cells [46–48], which also express ORP1L at relatively high levels. One can therefore envision that interaction of ORP1L with 7-ketocholesterol in this cell type may be of specific physiologic relevance in the context of atherogenesis. The finding that ORP1L binds 24(S)OHC is also of interest—besides macrophage, the ORP1L mRNA is most abundant in the central nervous system (CNS) [18, 49], and 24(S)OHC generated by CNS neurons plays a central role in maintaining the CNS sterol homeostasis [43, 50]. Detailed study of ORP1L function associated with these two newly identified oxysterol ligands is therefore a highly interesting topic for future investigations.

As also shown for OSBP [9], ORP9 [36], ORP2 [35] and *S. cerevisiae* Osh4p [33, 51], we provide here convincing evidence that ORP1L binds cholesterol. Since cholesterol is markedly more hydrophobic than the oxysterols tested, we could not compare its affinity for ORP1L in the charcoal–dextran binding assay employed to study binding of oxysterols. However, since cholesterol is far more abundant (typically more than four orders of magnitude) in cells than any of the oxysterols tested [52], we find it likely that cholesterol is a true physiologic ligand of ORP1L. In the case of OSBP, binding of 25OHC or cholesterol are known to have different functional consequences [9, 10]. While OSBP-cholesterol induces assembly of a protein phosphatase complex active on the extracellular signal regulated kinases (ERK), the complex is disassembled when 25OHC binds to OSBP. This could also be the case for ORP1L. The putative functional distinctions between oxysterol- and cholesterol-bound ORP1L remain to be elucidated in future studies.

Rocha et al. [30] used a truncated ORP1L (ORP1L ΔORD) lacking the entire sterol binding domain (more than 50% of the polypeptide) to shed light on the functional role of ORP1L ligand binding. They found out that, similarly to cellular cholesterol depletion, the expression of the truncated ORP1L results in a scattered distribution of LE. Their data also suggested that this is due to bridging by ORP1L between VAP proteins in the ER and Rab7 on LE, and that the VAPs may in this situation directly interact with dynein–dynactin motor complexes removing them from the LE surface. In the present study, we created a more specific sterol binding mutant with a 4-aa deletion in the lid of the sterol binding cavity, ORP1L Δ560–563. This mutant was shown to be stable, to have a severe defect in binding of several oxysterols, and to interact normally with Rab7. However, we were unable to establish whether it is also defective in cholesterol binding, since it behaved anomalously in the LUV cholesterol binding assay we used (data not shown), putatively due to an altered conformation of the sterol binding pocket lid, rich in hydrophobic amino acid residues. The mutant induced a scattered distribution of LE apparently analogous to that observed by Rocha et al. [30] for ORP1L ΔORD. Moreover, by disrupting the VAP binding FFAT motif in ORP1L Δ560–563, we provide strong evidence that the LE scattering observed with the sterol binding mutant indeed depends on the interaction of ORP1L with the ER VAP proteins. Thus, our data support the major conclusion of the Rocha et al. study.

The emphasis of LE/lysosome distribution in cells under normal culture conditions is in the perinuclear region, reflecting a tendency to move towards microtubule minus ends. Cholesterol depletion induces a shift of LE towards a peripheral distribution, and cholesterol accumulation leads to enhanced perinuclear clustering of late endocytic compartments, apparently via stabilization of GTP-Rab7 on the endosome limiting membrane [30, 53]. Overexpression of ORP1L sterol binding deficient mutants or the WT protein result in similar modifications of the endo-lysosome distribution. The effects of ORP1L overexpression help us grasp certain principles of ORP1L action and support the view that ORP1L plays a role in mediating the effects of cellular cholesterol status on LE/lysosome positioning.

However, the present experiments involving quantification of the actual LE motility, in addition to monitoring their positioning under conditions of ORP1L overexpression or silencing, add important new insight into the function of ORP1L. (1) They confirm that the endogenous ORP1L positively regulates LE/lysosome movement towards the microtubule minus ends; (2) the findings demonstrate that the presence of ORP1L is not required for a shift in LE motor protein balance towards plus-end directed activity, as suggested by Rocha et al. [30]; this is clearly shown by the increased peripheral location of the LE tracks in ORP1L silenced cells; and (3) the increased LE/lysosome motility in cells ORP1L silenced and their close to normal movement in cells overexpressing the ORP1L mFFAT mutant (as opposed to WT ORP1L) suggest that LE–ER contacts, facilitated by the interaction of ORP1L FFAT motif with VAP proteins in the ER, restrict LE motility.

The perinuclear LE clustering observed in cells expressing WT ORP1L or the Δ560–563 mFFAT double mutant is apparently an overexpression artefact caused by an as yet poorly understood process. Our data suggest that the clustering can be inhibited by two mechanisms: by stabilizing LE–ER interactions via inhibition of ORP1L sterol binding (the Δ560–563 mutant), which precludes motility and reduces the odds of LE coming into direct contact with each other, or by increasing the overall LE motility, which is capable of partially overriding the

clustering tendency. The regulation of LE motility through ORP1L–VAP interactions and the clustering may represent phenomena arising through different mechanisms. However, the clustering, when effective, strongly paralyzes LE motility. Sterol binding by ORP1L regulates the affinity of the protein for ER, as suggested by the Rocha et al. study [30], and our present data strongly support a close interaction of the VAP and sterol binding functions of ORP1L—the phenotype of the Δ560–563 mFFAT double mutant is strikingly different from either of the individual mutations.

We found that both WT ORP1L and the sterol binding-deficient mutant Δ560–563, inducing highly different distributions of the LE, recruited dynactin and kinesin 2 on the endosome surfaces. We therefore find it likely that the recruitment of microtubule-dependent motors is upstream of the regulation of ORP1L function by sterol binding. Further, our data are consistent with a model in which ORP1L sterol binding controls its affinity for VAP proteins, and one function of this interaction is a direct regulation of LE/lysosome motility. However, we find it difficult to believe that regulation of LE motility could be the only function of the ORP1L-induced LE–ER contacts. Membrane contact sites, junctions between the ER and other subcellular compartments, have been implicated in the inter-organelle transport of small compounds such as lipids or Ca^{2+} [26]. Moreover, a recent report demonstrates a role of contacts between the endosomes and the ER in the interaction of EGF receptor with a protein tyrosine phosphatase located in the ER [54]. There is also evidence for the function of *S. cerevisiae* ORPs in non-vesicular sterol transport through membrane contact sites [55], and the mammalian OSBP, ORP2, and ORP9 have been implicated in intracellular lipid transport [8, 36, 56], which could occur via such structures.

Our live cell imaging shows for the first time that ORP1L impacts the motility, not only the positioning of late endocytic compartments. Intriguingly, the motility of Alexa568-dextran labeled compartments carrying no detectable ORP1L on their surface was also reduced. We also found that the lysosomal degradation of internalized rhoEGF was markedly inhibited in cells overexpressing wild-type ORP1L or the sterol binding mutant. These observed disturbances could be explained by sequestration of factors necessary for LE dynamics/function, such as Rab7 or motor proteins. This is supported by the data of Johansson et al. [23] showing that GTP-bound Rab7 is stabilized on the surface of LE decorated by overexpressed ORP1L. The motor accumulation by ORP1L may occur via Rab7 stabilized on the LE and RILP, since no direct binding of dynactin or kinesin 2 by ORP1L was detected [27; this study].

ORP1L is abundant in macrophages [18] and its overexpression was shown to increase the size of atherosclerotic lesions in LDL receptor-deficient mice [42]. It was therefore of interest to study whether ORP1L silencing affects cholesterol efflux from macrophage foam cells, a process important for the development of atherosclerotic lesions. Experiments carried out on RAW264.7 macrophages subjected to lentiviral ORP1L silencing showed that reduction of cellular ORP1L significantly inhibited cholesterol efflux to apolipoprotein A-I but not to spherical HDL particles. The acceptor selectivity of the effect suggests that the observed inhibition is related to the function of ABCA1, which mediates cholesterol efflux to poorly lipidated apoA-I [57]. This together with the finding that inhibition of cholesterol efflux was not detected when free [^{3}H]cholesterol was used for labeling suggests that the ORP1L effect is specific for cholesterol originating from endocytic lipoprotein uptake. Consistent with our findings and interpretation, ABCA1 plays a key role in removing cholesterol from the endo-lysosomal compartments of cells with lipoprotein-derived cholesterol accumulation [58, 59]. The precise mechanism of how ORP1L silencing impairs cholesterol efflux remains open, but may be indirect, possibly via the ORP1L-controlled endosome motility.

In summary, the present data demonstrate that not only the positioning of LE but also endosome motility and their functions in both protein and lipid transport are regulated by ORP1L and its ligand binding status. These observations provide a basis for future identification of the molecular complexes ORP1L is part of, and for understanding the principles through which sterol signals are interpreted to control late endocytic events and lipid fluxes. Furthermore, our findings underscore the importance of elucidating the role of endogenous macrophage ORP1L in atherosclerotic lesion development.

Acknowledgments We are grateful to Lea Puhakka, Seija Puomilahti and Pirjo Ranta for skilled technical assistance, Jaakko Ilola for skilled assistance in endosome motility quantitation, and to Drs. Matti Jauhiainen and Marianna Maranghi for the lipoprotein preparations. Dr. Jacques Neefjes (The Netherlands Cancer Institute, Amsterdam) is thanked for kindly providing the GFP-RILP cDNA construct. This study was supported by the Minerva Foundation (Helsinki), the Sigrid Juselius Foundation, the Academy of Finland (grant 121457 to V.M.O. and 131429 to E.I.), the Finnish Foundation for Cardiovascular Research, the Magnus Ehrnrooth Foundation, the European Union FP7 (LipidomicNet, agreement no. 202272), the Finnish Concordia Fund (T.V.), and the Finnish Atherosclerosis Society (T.V.). Terhi Vihervaara is a member of Helsinki Biomedical Graduate School. Riikka-Liisa Uronen is a member of Helsinki Graduate School in Biotechnology and Molecular Biology.

References

1. Taylor FR, Saucier SE, Shown EP, Parish EJ, Kandutsch AA (1984) Correlation between oxysterol binding to a cytosolic

binding protein and potency in the repression of hydroxymethylglutaryl coenzyme A reductase. J Biol Chem 259:12382–12387
2. Dawson PA, Ridgway ND, Slaughter CA, Brown MS, Goldstein JL (1989) cDNA cloning and expression of oxysterol-binding protein, an oligomer with a potential leucine zipper. J Biol Chem 264:16798–16803
3. Dawson PA, Van der Westhuyzen DR, Goldstein JL, Brown MS (1989) Purification of oxysterol binding protein from hamster liver cytosol. J Biol Chem 264:9046–9052
4. Wyles JP, McMaster CR, Ridgway ND (2002) Vesicle-associated membrane protein-associated protein-A (VAP-A) interacts with the oxysterol-binding protein to modify export from the endoplasmic reticulum. J Biol Chem 277:29908–29918
5. Levine TP, Munro S (1998) The pleckstrin homology domain of oxysterol-binding protein recognises a determinant specific to Golgi membranes. Curr Biol 8:729–739
6. Levine TP, Munro S (2002) Targeting of Golgi-specific pleckstrin homology domains involves both PtdIns 4-kinase-dependent and -independent components. Curr Biol 12:695–704
7. Roy A, Levine TP (2004) Multiple pools of phosphatidylinositol 4-phosphate detected using the pleckstrin homology domain of Osh2p. J Biol Chem 279:44683–44689
8. Perry RJ, Ridgway ND (2006) Oxysterol-binding protein and vesicle-associated membrane protein-associated protein are required for sterol-dependent activation of the ceramide transport protein. Mol Biol Cell 17:2604–2616
9. Wang PY, Weng J, Anderson RG (2005) OSBP is a cholesterol-regulated scaffolding protein in control of ERK 1/2 activation. Science 307:1472–1476
10. Wang PY, Weng J, Lee S, Anderson RG (2008) The N terminus controls sterol binding while the C terminus regulates the scaffolding function of OSBP. J Biol Chem 283:8034–8045
11. Yan D, Olkkonen VM (2008) Characteristics of oxysterol binding proteins. Int Rev Cytol 265:253–285
12. Raychaudhuri S, Prinz WA (2010) The diverse functions of oxysterol-binding proteins. Annu Rev Cell Dev Biol. doi: 10.1146/annurev.cellbio.042308.113334
13. Ridgway ND (2010) Oxysterol-binding proteins. Subcell Biochem 51:159–182
14. Lehto M, Laitinen S, Chinetti G, Johansson M, Ehnholm C, Staels B, Ikonen E, Olkkonen VM (2001) The OSBP-related protein family in humans. J Lipid Res 42:1203–1213
15. Jaworski CJ, Moreira E, Li A, Lee R, Rodriguez IR (2001) A family of 12 human genes containing oxysterol-binding domains. Genomics 78:185–196
16. Anniss AM, Apostolopoulos J, Dworkin S, Purton LE, Sparrow RL (2002) An oxysterol-binding protein family identified in the mouse. DNA Cell Biol 21:571–580
17. Beh CT, Cool L, Phillips J, Rine J (2001) Overlapping functions of the yeast oxysterol-binding protein homologues. Genetics 157:1117–1140
18. Johansson M, Bocher V, Lehto M, Chinetti G, Kuismanen E, Ehnholm C, Staels B, Olkkonen VM (2003) The two variants of oxysterol binding protein-related protein-1 display different tissue expression patterns, have different intracellular localization, and are functionally distinct. Mol Biol Cell 14:903–915
19. Lehto M, Tienari J, Lehtonen S, Lehtonen E, Olkkonen VM (2004) Subfamily III of mammalian oxysterol-binding protein (OSBP) homologues: the expression and intracellular localization of ORP3, ORP6, and ORP7. Cell Tissue Res 315:39–57
20. Ridgway ND, Dawson PA, Ho YK, Brown MS, Goldstein JL (1992) Translocation of oxysterol binding protein to Golgi apparatus triggered by ligand binding. J Cell Biol 116:307–319
21. Wyles JP, Ridgway ND (2004) VAMP-associated protein-A regulates partitioning of oxysterol-binding protein-related protein-9 between the endoplasmic reticulum and Golgi apparatus. Exp Cell Res 297:533–547
22. Lehto M, Hynynen R, Karjalainen K, Kuismanen E, Hyvärinen K, Olkkonen VM (2005) Targeting of OSBP-related protein 3 (ORP3) to endoplasmic reticulum and plasma membrane is controlled by multiple determinants. Exp Cell Res 310:445–462
23. Johansson M, Lehto M, Tanhuanpää K, Cover TL, Olkkonen VM (2005) The oxysterol-binding protein homologue ORP1L interacts with Rab7 and alters functional properties of late endocytic compartments. Mol Biol Cell 16:5480–5492
24. Loewen CJ, Roy A, Levine TP (2003) A conserved ER targeting motif in three families of lipid binding proteins and in Opi1p binds VAP. EMBO J 22:2025–2035
25. Olkkonen VM, Levine TP (2004) Oxysterol binding proteins: in more than one place at one time? Biochem Cell Biol 82:87–98
26. Levine T, Loewen C (2006) Inter-organelle membrane contact sites: through a glass, darkly. Curr Opin Cell Biol 18:371–378
27. Johansson M, Rocha N, Zwart W, Jordens I, Janssen L, Kuijl C, Olkkonen VM, Neefjes J (2007) Activation of endosomal dynein motors by stepwise assembly of Rab7-RILP-p150Glued, ORP1L, and the receptor betalll spectrin. J Cell Biol 176:459–471
28. Jordens I, Fernandez-Borja M, Marsman M, Dusseljee S, Janssen L, Calafat J, Janssen H, Wubbolts R, Neefjes J (2001) The Rab7 effector protein RILP controls lysosomal transport by inducing the recruitment of dynein–dynactin motors. Curr Biol 11:1680–1685
29. Cantalupo G, Alifano P, Roberti V, Bruni CB, Bucci C (2001) Rab-interacting lysosomal protein (RILP): the Rab7 effector required for transport to lysosomes. EMBO J 20:683–693
30. Rocha N, Kuijl C, van der Kant R, Janssen L, Houben D, Janssen H, Zwart W, Neefjes J (2009) Cholesterol sensor ORP1L contacts the ER protein VAP to control Rab7-RILP-p150 Glued and late endosome positioning. J Cell Biol 185:1209–1225
31. Johansson M, Olkkonen VM (2005) Assays for interaction between Rab7 and oxysterol binding protein related protein 1L (ORP1L). Methods Enzymol 403:743–758
32. Thompson JD, Higgins DG, Gibson TJ (1994) CLUSTAL W: improving the sensitivity of progressive multiple sequence alignment through sequence weighting, position-specific gap penalties and weight matrix choice. Nucleic Acids Res 22:4673–4680
33. Im YJ, Raychaudhuri S, Prinz WA, Hurley JH (2005) Structural mechanism for sterol sensing and transport by OSBP-related proteins. Nature 437:154–158
34. Berman H, Henrick K, Nakamura H (2003) Announcing the worldwide Protein Data Bank. Nat Struct Biol 10:980
35. Hynynen R, Suchanek M, Spandl J, Back N, Thiele C, Olkkonen VM (2009) OSBP-related protein 2 is a sterol receptor on lipid droplets that regulates the metabolism of neutral lipids. J Lipid Res 50:1305–1315
36. Ngo M, Ridgway ND (2009) Oxysterol binding protein-related Protein 9 (ORP9) is a cholesterol transfer protein that regulates Golgi structure and function. Mol Biol Cell 20:1388–1399
37. Basu SK, Goldstein JL, Anderson GW, Brown MS (1976) Degradation of cationized low density lipoprotein and regulation of cholesterol metabolism in homozygous familial hypercholesterolemia fibroblasts. Proc Natl Acad Sci USA 73:3178–3182
38. Brown MS, Dana SE, Goldstein JL (1975) Receptor-dependent hydrolysis of cholesteryl esters contained in plasma low density lipoprotein. Proc Natl Acad Sci USA 72:2925–2929
39. Perttilä J, Merikanto K, Naukkarinen J, Surakka I, Martin NW, Tanhuanpää K, Grimard V, Taskinen MR, Thiele C, Salomaa V, Jula A, Perola M, Virtanen I, Peltonen L, Olkkonen VM (2009) OSBPL10, a novel candidate gene for high triglyceride trait in dyslipidemic Finnish subjects, regulates cellular lipid metabolism. J Mol Med 87:825–835

40. Yan D, Mäyränpää MI, Wong J, Perttilä J, Lehto M, Jauhiainen M, Kovanen PT, Ehnholm C, Brown AJ, Olkkonen VM (2008) OSBP-related protein 8 (ORP8) suppresses ABCA1 expression and cholesterol efflux from macrophages. J Biol Chem 283:332–340
41. Suchanek M, Hynynen R, Wohlfahrt G, Lehto M, Johansson M, Saarinen H, Radzikowska A, Thiele C, Olkkonen VM (2007) The mammalian oxysterol-binding protein-related proteins (ORPs) bind 25-hydroxycholesterol in an evolutionarily conserved pocket. Biochem J 405:473–480
42. Yan D, Jauhiainen M, Hildebrand RB, Willems van Dijk K, Van Berkel TJ, Ehnholm C, Van Eck M, Olkkonen VM (2007) Expression of human OSBP-related protein 1L in macrophages enhances atherosclerotic lesion development in LDL receptor-deficient mice. Arterioscler Thromb Vasc Biol 27:1618–1624
43. Xu Y, Liu Y, Ridgway ND, McMaster CR (2001) Novel members of the human oxysterol-binding protein family bind phospholipids and regulate vesicle transport. J Biol Chem 276:18407–18414
44. Wyles JP, Perry RJ, Ridgway ND (2007) Characterization of the sterol-binding domain of oxysterol-binding protein (OSBP)-related protein 4 reveals a novel role in vimentin organization. Exp Cell Res 313:1426–1437
45. Brown CL, Maier KC, Stauber T, Ginkel LM, Wordeman L, Vernos I, Schroer TA (2005) Kinesin-2 is a motor for late endosomes and lysosomes. Traffic 6:1114–1124
46. Garcia-Cruset S, Carpenter KL, Guardiola F, Stein BK, Mitchinson MJ (2001) Oxysterol profiles of normal human arteries, fatty streaks and advanced lesions. Free Radic Res 35:31–41
47. Maor I, Kaplan M, Hayek T, Vaya J, Hoffman A, Aviram M (2000) Oxidized monocyte-derived macrophages in aortic atherosclerotic lesion from apolipoprotein E-deficient mice and from human carotid artery contain lipid peroxides and oxysterols. Biochem Biophys Res Commun 269:775–780
48. Vaya J, Aviram M, Mahmood S, Hayek T, Grenadir E, Hoffman A, Milo S (2001) Selective distribution of oxysterols in atherosclerotic lesions and human plasma lipoproteins. Free Radic Res 34:485–497
49. Laitinen S, Olkkonen VM, Ehnholm C, Ikonen E (1999) Family of human oxysterol binding protein (OSBP) homologues. A novel member implicated in brain sterol metabolism. J. Lipid Res 40:2204–2211
50. Björkhem I (2007) Rediscovery of cerebrosterol. Lipids 42:5–14
51. Raychaudhuri S, Im YJ, Hurley JH, Prinz WA (2006) Nonvesicular sterol movement from plasma membrane to ER requires oxysterol-binding protein-related proteins and phosphoinositides. J Cell Biol 173:107–119
52. Brown AJ, Jessup W (1999) Oxysterols and atherosclerosis. Atherosclerosis 142:1–28
53. Lebrand C, Corti M, Goodson H, Cosson P, Cavalli V, Mayran N, Faure J, Gruenberg J (2002) Late endosome motility depends on lipids via the small GTPase Rab7. EMBO J 21:1289–1300
54. Eden ER, White IJ, Tsapara A, Futter CE (2010) Membrane contacts between endosomes and ER provide sites for PTP1B-epidermal growth factor receptor interaction. Nat Cell Biol 12:267–272
55. Schulz TA, Choi MG, Raychaudhuri S, Mears JA, Ghirlando R, Hinshaw JE, Prinz WA (2009) Lipid-regulated sterol transfer between closely apposed membranes by oxysterol-binding protein homologues. J Cell Biol 187:889–903
56. Hynynen R, Laitinen S, Käkelä R, Tanhuanpää K, Lusa S, Ehnholm C, Somerharju P, Ikonen E, Olkkonen VM (2005) Overexpression of OSBP-related protein 2 (ORP2) induces changes in cellular cholesterol metabolism and enhances endocytosis. Biochem J 390:273–283
57. Yvan-Charvet L, Wang N, Tall AR (2010) Role of HDL, ABCA1, and ABCG1 transporters in cholesterol efflux and immune responses. Arterioscler Thromb Vasc Biol 30:139–143
58. Chen W, Sun Y, Welch C, Gorelik A, Leventhal AR, Tabas I, Tall AR (2001) Preferential ATP-binding cassette transporter A1-mediated cholesterol efflux from late endosomes/lysosomes. J Biol Chem 276:43564–43569
59. Azuma Y, Takada M, Shin HW, Kioka N, Nakayama K, Ueda K (2009) Retroendocytosis pathway of ABCA1/apoA-I contributes to HDL formation. Genes Cells 14:191–204